

# Locating and quantifying damage in deck type arch bridges using frequency response functions and artificial neural networks

N. Jayasundara<sup>1</sup>, D.P. Thambiratnam<sup>2</sup>, T.H.T. Chan<sup>2</sup>, A. Nguyen<sup>3</sup>

<sup>1</sup> Queensland University of Technology – Australia, Email: [walpola.jayasundara@hdr.qut.edu.au](mailto:walpola.jayasundara@hdr.qut.edu.au) <sup>2</sup> Queensland University of Technology – Australia, <sup>3</sup>University of Southern Queensland – Australia

## **Abstract:**

Vibration based methods can be used to detect damage in a structure as its vibration characteristics change with physical changes in the structure. Arch bridge is a popular type of bridge with rather complex vibration characteristics which pose a challenge for using existing vibration based methods to detect damage in the bridge. Further, its particular geometry with a curved arch rib and vertical members (either in compression or tension) to support the horizontal deck makes the process of damage quantification using vibration based methods harder and challenging. This paper develops and presents a vibration-based method that utilizes damage pattern changes in frequency response functions (FRFs) and artificial neural networks (ANNs) to locate and quantify damage in the rib of deck-type arch bridge, which is the most important load bearing component in the bridge. Principal component analysis, which is performed to reduce the dimension of original FRF data series and to obtain limited PCA-compressed FRF data is used in the development of the proposed method. FRF change, which is the difference in the FRF data between the intact and the damaged structure, is compressed to a few principal components and fed to ANNs to predict the location and severity of structural damage. The process and the hierarchy of developed ANN systems are presented, including the ‘fusion network’ concept, which individually analyses FRF-based damage indicators separated by sensor locations. Finally, results obtained for many tested damage cases (inverse problems) are presented, which demonstrate the applicability of the proposed method for locating and quantifying damage in the rib of deck type arch bridge.

## **Keywords**

Bridge failure; Arch bridge; Vibration based damage detection (VBDD); Artificial neural networks (ANN); Frequency Response Functions; Principal Component Analysis

## **1. Introduction**

It is evitable for civil structures to gradually accumulate damage due to various causes such as environmental changes, material aging, variation of load characteristics, inadequate

maintenance etc. These structures need to be monitored, especially those that are aging, so that any damage is detected at the onset and appropriate retrofitting carried out to ensure that they are capable of providing safe and reliable service without unexpected failures. Research in this area has attracted much attention over the years and there has been considerable amount of research on damage detection in simple and complex structures which includes beams<sup>1-4</sup>, plate elements<sup>5,6</sup>, trusses<sup>7-10</sup>, offshore platforms<sup>11</sup>, bridges<sup>12-15</sup>, full scale buildings<sup>16-18</sup> etc.

Vibration-based damage detection (VBDD) techniques can be classified as global methods<sup>19</sup> which examine the changes in vibration properties between the healthy and damaged states of the structure to evaluate the damage. Modal parameter based approaches such as natural frequency based methods, mode shape based methods, modal flexibility method and modal strain energy method have been some of the commonly used methods. However, these methods are often sensitive to incomplete modal data, demand a number of data acquisition locations and less reliable with environmental noise contamination. In contrast, direct use of output only modal analyses have several advantages compared to modal parameter based methods<sup>20</sup>. Frequency Response Function (FRF) is such method with many advantages over traditional VBDD methods. FRFs are one of the easiest to obtain real-time data which requires only a small number of sensors and very little human involvement<sup>21</sup>. FRFs can be recognised as normalised complex quantities that specify how vibration is transmitted as a function of frequency between points on the structure. Measured FRFs provide a compact form of data obtained from vibration tests of structures and provide adequate information on the structure's dynamic behaviour for a considerable number of degrees of freedom and over a range of frequencies<sup>22</sup>. FRF based damage detection techniques do not require post data analysis as in experimental modal analysis and thus prevent human errors and extended times to process. Similar to modal parameters, FRF data are sensitive to structural changes and hence can be used as an indicator to detect structural damage. Applications of FRF in damage detection and severity estimation has quite a long history<sup>23-25</sup>. The difference between FRF data collected from damaged and non-damaged structures has revealed promising results in damage detection studies<sup>26</sup>. It was found that the residual FRF concept provides an enhanced damage fingerprint and thereby improves the damage detection possibilities<sup>27</sup>.

However there remain some unaddressed problems related to the use of FRF in damage identification. These include complex behaviour and large number of unknown parameters in complex structures, robustness of damage identification algorithms to measurement noise and errors, limited number of measurement sensors and incomplete data sets, accuracy and

reliability in identification of damage location and severity, detection of small size damages and multiple damages. Therefore, this study focused on developing a method which can effectively utilize the FRF to obtain effective solutions to above mentioned problems.

ANN is a machine learning method which is capable of pattern recognition, classification, self-organizing and nonlinear modelling<sup>28-30</sup>. A well trained neural network is capable of extracting and obtaining precise and reliable information from imprecise, unreliable, inconsistent, uncertain, and noise-polluted data<sup>31</sup> and train itself to provide accurate outputs to given unknown inputs. The robust pattern recognition, classification and fitting abilities of Artificial Neural Networks (ANNs) can be advantageously utilised with some effective output data types to detect the damage characteristics (location and severities). Derivatives of model data<sup>32,33</sup>, FRF and Wavelet Transform (WT)<sup>34,35</sup> were identified as powerful analytical tools to capture dynamic features of inputs and outputs of the structures and these methods have been widely used along with ANN over the past decades in damage identification processes of structures; specially multi storey buildings. Therefore, these methods eventually became the input data for neural network training performed towards damage identification of structures.

The ability of ANN to effectively extract the patterns hidden in large amount of data and train itself to identify similar behaviour is the key feature that is used in this study to address the limitations of FRF discussed above (to detect and quantify damage). Thus, FRF was used along with ANN to produce an effective damage identification tool for arch bridges.

FRF data obtained for a specific frequency range can be massive, containing a large number of data points. Therefore, using the full FRF spectra on ANNs will demand a large number of input nodes, which can ultimately cause problems in convergence and computational efficiencies. On the other hand, the selection of partial or random data ranges may cause loss of information and incorrect results<sup>36</sup>. Principal Component Analysis (PCA) has been found to be a useful tool for dimension reduction (section) in large data sets. Converting the important features of the original data set into PCs can significantly reduce its size without diluting the important features. Furthermore, PCA can also be recognized as a powerful tool in reducing the effect of measurement noise and random uncertainties.

FRF data is usually extracted from a single location of a structure. The direct use of these FRFs may be misleading when that particular location is neither damaged nor sensitive to damage in nearby places. On the other hand, measurement noise also has different effects on FRF data at different points of a structure. Thus, the distance between the damage and data collection point is a critical factor when identifying unknown damage. Analysing several FRF

data series collected from different locations on the structure separately in individual neural networks will therefore help to identify the unique characteristics from different sensor signals. Finally, fusing those different network outcomes to a single network to obtain a single output is found to be the best way to obtain optimum results.

The proposed method for damage prediction in the rib of arch bridges utilises the residual FRFs (the difference between the FRFs of intact and damaged structures) as the base for damage identification algorithm. The changing patterns of residual FRFs that represent the unique damage fingerprints sensitive to damage location and severity can be analysed by artificial neural network (ANN), a machine learning technique which can train itself to provide accurate outputs to given unknown inputs. To obtain a better convergence and hence more accurate damage detection results, the residual FRFs are compressed into principal components (PCs) using principal component analysis (PCA). The hierarchy of individual networks and its fusion are designed to take advantage of different characteristics of sensor locations, and thereby a more robust and efficient damage identification method is obtained.

This paper combines FRF and PCA with artificial neural network (ANN) technology to develop and apply a method to locate and quantify damage in the rib of an arch bridge which is the most important load bearing structural component in the bridge. ANN is a machine learning method which is capable of pattern recognition, classification, self-organizing and nonlinear modelling<sup>28-30</sup>. A well trained neural network is capable of extracting and obtaining precise and reliable information from imprecise, unreliable, inconsistent, uncertain, and noise-polluted data<sup>31</sup> and train itself to provide accurate outputs to given unknown inputs.

The application of Damage Indices (DIs) based on vibration data with ANN to quantify damage is limited in the literature and hardly applied to full scale structures. There are some studies on detecting and quantifying damage in beams<sup>37</sup>, frames<sup>32</sup>, multi storey building models<sup>38</sup> and bridge models<sup>33,39-41</sup> using both FRF and ANN. Most recent research based on neural network technology provides the evidence that the neural network- frequency response function combination is an effective technique to be used in damage detection<sup>31,42</sup>.

To illustrate the applicability of the proposed damage detection technique to a full scale long span arch bridge, a complete finite element model of the 213m long Cold Spring Canyon Bridge in the US was developed and validated<sup>43</sup>. A number of damage scenarios on the arch rib are treated and the results demonstrate the capability of the proposed method to locate and quantify damage in the ribs of the arch bridges.

## 2. Methodology

This paper develops and applies a vibration-based method to locate and quantify damage in the arch rib of a long span arch bridge using residual FRFs and ANNs. The FRFs obtained from the structure are the basic data collected for damage recognition and further analyses. However, the FRFs need to be processed in a way to filter the changes caused by any anomalies in the structure. Therefore, Residual FRFs were calculated as the second phase of the process and this step is explained in Section 2.2. These Residual FRFs contain large amount of data which can make the pattern recognition process harder for ANNs. Therefore, to obtain suitable input data for network training, the residual FRFs are compressed to a few PCs adopting PCA techniques. PCA is a dimensionality reduction and data compression tool which can be ideally used to compress the FRF data without missing any important information in it. This process is elaborated in Section 2.3.

Thereafter the PCA compressed residual FRFs were used as inputs to the Neural network to recognize the damage location and severity. A hierarchy of neural networks utilized the different characteristics obtained by individual measurements from different sensor locations. The method is tested on compressed and normalized and non-normalized residual FRF data. To investigate the robustness of the developed method to noise, a noise sensitivity study examining four different noise pollution levels is conducted for the numerical data. This process is elaborated in Section 3.

Moreover, the above mentioned process can be summarized as follows. Firstly, FRFs are calculated from the time history data obtained through finite element (FE) analysis of the bridge models and then residual FRFs are obtained by computing FRF differences between the undamaged and the damaged arched rib. Thirdly, by adopting PCA techniques, the residual FRFs are compressed and the most important PCs identified. Fourthly, sets of individual sensor neural networks are trained and tested with PCA-compressed residual FRFs separated by measurement locations. Finally, a neural network ensemble fuses the outcomes of the individual networks and an overall damage prediction is obtained. This process can be explained through the flow chart as shown below in Figure 1.

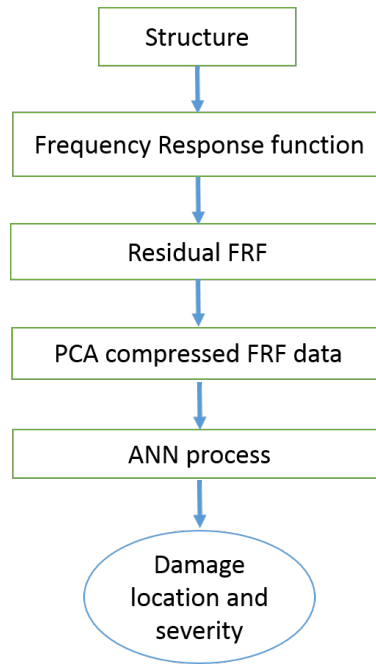


Figure 1: Damage detection process

## 2.1 Cold Canyon Bridge

To illustrate the applicability of the proposed damage prediction technique to a full-scale long-span arch bridge, a complete FE model of the Cold Spring Canyon Bridge is developed using ABAQUS FE modelling software (Figure 2). The Cold Spring Canyon Bridge is a long-span, deck type steel arch bridge with a span of 213 m and a rise of 36.27m. The validation of the FE model of this bridge and the applicability of the modified vibration based damage indices (DIs) to detect and locate damage in this bridges have been presented in <sup>43</sup>.

To evaluate the performance of the proposed method, damage was introduced as percentage stiffness reductions at small regions along the arch rib. All the damaged locations are referred to their X coordinates, considering the origin at the left end of the arch rib.



Figure 2: (a) Real Cold Canyon Bridge (b) Finite element model of the bridge

## 2.2 Residual Frequency Response Function

FRF of a structure is sensitive to its structural anomalies. Damage can alter the amplitudes and the shapes of the original FRFs of the structural elements. This characteristic is successfully utilised in this study to identify unknown damages in the structure. Residual FRF is generated as the first step in the preparation of data to build damage detection and quantification algorithms. The residual FRF defined by Dackermann<sup>27</sup> is as follows:

$$ResH(\omega) = H_d(\omega) - H_h(\omega) \quad \text{Equation 1}$$

$H_d(\omega)$  and  $H_h(\omega)$  are FRF data obtained from the damaged and undamaged structure respectively.

Figure 3 presents 5 random damage locations selected along the length of the arch rib for applying the proposed damage prediction method.

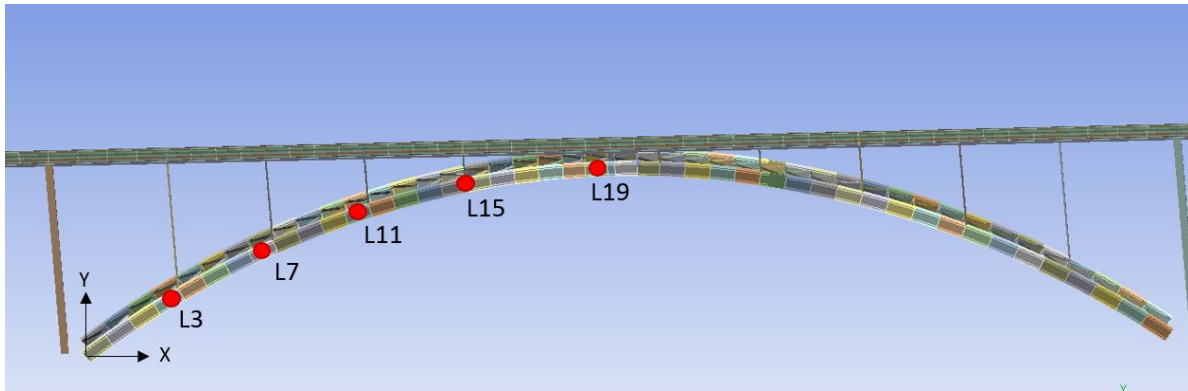


Figure 3: Damage locations on the rib of the arch bridge

Figure 4 and Figure 5 present the residual FRFs obtained from the arch rib of the Cold Canyon Bridge for different damage severities and different damage locations on the rib under 1% noise contamination. Figure 4 shows the variation of FRF under different severities at the same damage location. 5%, 10%, 15% and 20% stiffness reductions were applied at the location X= 37m (L3 in Figure 3) and the residual FRF curves were obtained. The graphs confirm that the increase in damage severity increases the amplitudes of the peaks. Further, Figure 5 presents the variation of FRF with the damage location on the rib under the same severity; which is 15% stiffness reduction. Damages were applied at location numbers L5, L10, L15 and L20 and residual FRFs were obtained. Even though all the FRFs follow a common overall pattern, the damage location influences the pattern and the peak heights of the individual FRFs. For instance, at 3.2Hz the highest peak is indicated for the L15 damage FRF while at 4.6Hz the highest peak shows L20 damage FRF. Furthermore, it is noted that FRF values closest to the

peaks are mostly affected by damage; which simply means the resonant frequencies are affected by the damages.

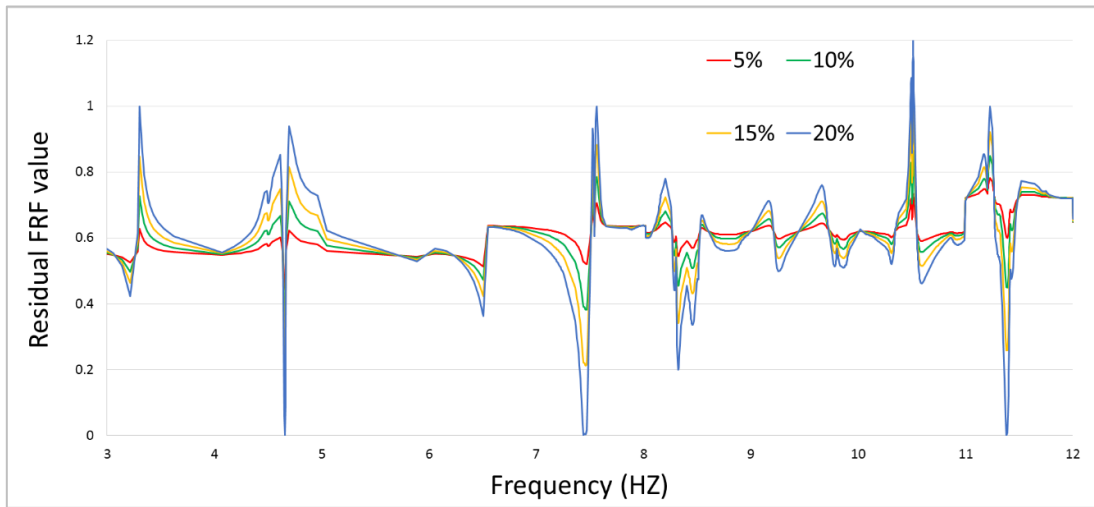


Figure 4: Variation of residual FRFs for different damage severities at location 03 (constant location)

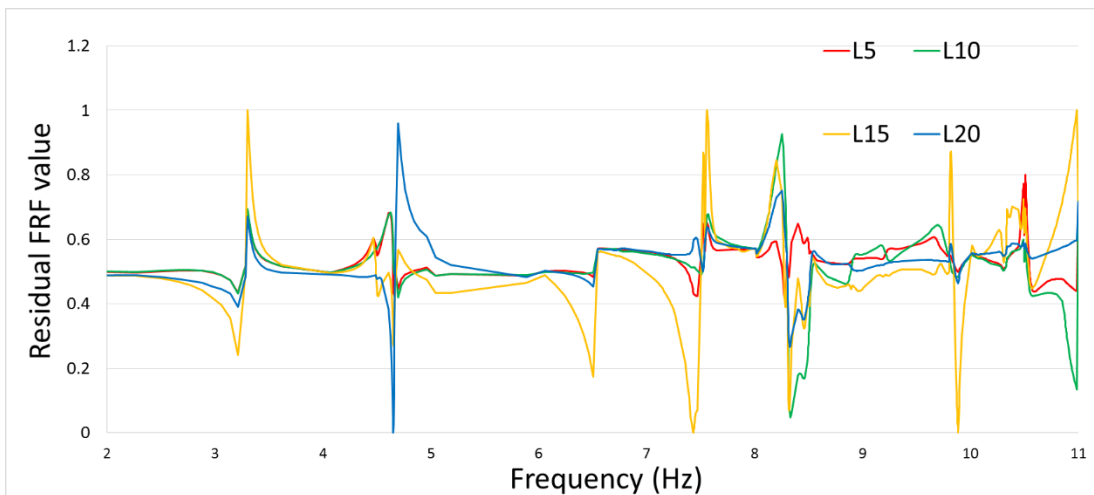


Figure 5: Variation of residual FRFs for different damage locations under constant damage severity

The direction of FRF is another important factor of concern. Figure 4 and Figure 5 present the FRFs extracted from the longitudinal direction; hence, the longitudinal modes are captured. This may cause the important details of the torsional and vertical modes to be missed and hence not recorded in the FRF data. As a preventive measure, this study uses FRFs from each of the three directions (longitudinal, vertical and transverse) separately so that the damage characteristics pertaining to all the 3 directions will be captured. The characteristics of residual FRFs such as varying shapes, altering amplitudes and shifting peaks with the damage location

and severities are used effectively in ANN training so that the trained network is capable of recognising the exact damage location with the severity of unknown damage.

### **2.3 Principal Component Analysis for Frequency Response Function**

FRF data for a certain frequency range contains a large number of data points which can cause problems when processing at ANNs. One directional (X, Y or Z) full spectrum (full residual FRF curve) for a frequency range of 0Hz to 20Hz, contains 1485 points which can be considered as 1485 input variables for the neural network. The full spectrum of 3 directions therefore contains 4455 input points which is comparatively a high number to be used as input variables for 720 cases (the total number of different damage cases considered). Therefore, to obtain more reliable output from ANN, and to train the network without convergence or processing time limitations, the input variables (data points) obtained from residual FRFs need to be reduced. Principal Component Analysis (PCA) is hence adopted as a method to reduce the size of the whole spectrum and to filter the noise. PCA is a dimensionality reduction and data compression tool which can be ideally used to compress the FRF data without missing any important information in it. The residual FRF data are then converted to Principal Components (PCs) using MATLAB 'pca' function.

PCA was performed on normalized data to not to give emphasis to those variables that have higher variances than to those that have lower variances. The first PC represents most information in the original data set and the second PC represents the second most important features and therefore, the last PC contains a minimal amount of information. It is important to determine the optimum number of PCs which represent the maximum amount of information. In general, determination of optimum number of PCs depends on the quality of the damage patterns represented by the data set and the level of noise<sup>27</sup>. It is recommended to do a sensitivity study on the PC contributions of damage characteristics and noise levels to identify the optimum number of PCs. Generally, indications of the dominant features of a data set are given by individual and cumulative contributions of PCs. For instance, if the first 20 PCs represent more than 99% of the information of the original data, then a selection of more than 20 PCs for damage prediction is unnecessary as the information retrieved by higher PCs will be negligible.

In this study, 4455 variables were converted to PCs and the individual contributions of the first few PCs are presented in Table 1 (3 direction FRFs of 5 locations and summation). It is noted that the first few PCs have the highest contribution to represent information of whole FRF

spectrum. Since the first 25 PCs contribute to 99% of total information, the first 25 PCs were selected as input variables to neural networks.

Table 1: Contribution of first 25 PCs for 6 location cases (Normalised data)

PC\Location	1	2	3	4	5	Sum
PC1	56.28	42.38	40.91	34.99	37.18	40.60
PC2	18.79	21.89	17.46	22.35	24.83	29.07
PC3	7.29	14.24	15.21	15.72	11.73	11.27
PC4	3.86	6.53	8.31	9.22	8.23	6.78
PC5	2.79	3.94	5.52	3.75	4.02	3.12
PC6	2.11	3.05	3.16	3.57	3.32	2.21
PC7	1.47	1.88	1.97	2.48	2.64	1.58
PC8	1.18	1.62	1.89	1.75	1.42	1.05
PC9	0.98	1.00	1.27	1.34	1.04	0.90
PC10	0.81	0.83	1.00	0.98	0.87	0.81
PC11	0.68	0.45	0.80	0.71	0.74	0.62
PC12	0.59	0.28	0.58	0.65	0.71	0.43
PC13	0.48	0.23	0.40	0.47	0.50	0.33
PC14	0.43	0.22	0.30	0.31	0.43	0.28
PC15	0.36	0.20	0.21	0.29	0.36	0.14
PC16	0.28	0.14	0.18	0.21	0.32	0.11
PC17	0.23	0.13	0.14	0.18	0.27	0.10
PC18	0.18	0.12	0.13	0.15	0.19	0.07
PC19	0.17	0.10	0.08	0.14	0.17	0.07
PC20	0.13	0.09	0.07	0.10	0.15	0.06
PC21	0.11	0.08	0.06	0.09	0.12	0.05
PC22	0.10	0.07	0.05	0.08	0.11	0.05
PC23	0.09	0.06	0.04	0.07	0.08	0.04
PC24	0.07	0.05	0.03	0.05	0.07	0.03
PC25	0.07	0.04	0.03	0.04	0.06	0.02
$\sum_{1}^{25} PC$	99.54	99.62	99.83	99.68	99.57	99.8

Damage makes the FRF deviate from its healthy state and hence creates a difference between the healthy FRF and damaged FRF. Higher the damage, higher the difference between healthy

and damaged state FRFs (Figure 4). This feature is expected to be used advantageously for the quantification process. However, normalising all the data for PCA makes the above mentioned FRF difference (caused by different severities) invisible and hence makes it hard or nearly impossible to use in the damage quantification process. On the other hand, PCA on non-normalised (original) data creates skewed or biased PCs, which are not perfect for ANN analyses. To minimise the disadvantage caused by non-normalized PCs and to maximise the accuracy of damage quantification, two-stage locating and quantifying process is proposed.

To achieve the above mentioned objective, two principal component analyses (PCAs) were conducted separately with normalised and non-normalized data and these PCs are used in two stage neural network system to obtain the maximum convergence and optimum results from neural networks. PCs obtained from normalised data are utilised in the classification neural network while the PCs obtained from non-normalized data are used in the fitting network. The first 25 PCs were selected from normalised FRFs as the inputs for classification neural network and first 15 PCs were selected from non-normalized PCs as the inputs for the fitting neural network. Table 2 below shows the individual contributions of the first 15 PCs obtained from non-normalized FRF data (FRFs of 5 locations and summation). Since the first 15 PCs contribute to 99.9% of total information of whole FRF spectra, first 15 PCs were selected as input variables to the fitting neural network.

Table 2: Contribution of first 15 PCs for 6 location cases (Non-normalised data)

PC\Location	1	2	3	4	5	Sum
PC1	83.30	89.81	76.84	79.46	49.08	65.89
PC2	11.32	5.36	14.48	9.38	40.51	10.20
PC3	3.57	2.52	4.08	3.65	5.98	9.36
PC4	1.23	1.45	1.97	3.10	1.93	8.32
PC5	0.26	0.35	1.92	2.10	1.08	2.45
PC6	0.14	0.22	0.26	1.08	0.72	2.01
PC7	0.07	0.10	0.13	0.59	0.24	1.06
PC8	0.05	0.08	0.12	0.25	0.17	0.26
PC9	0.02	0.05	0.06	0.17	0.09	0.15
PC10	0.01	0.02	0.05	0.08	0.06	0.12
PC11	0.01	0.01	0.02	0.04	0.05	0.06
PC12	0.01	0.01	0.01	0.03	0.03	0.04

PC13	0.00	0.01	0.01	0.02	0.01	0.02
PC14	0.00	0.00	0.01	0.01	0.01	0.02
PC15	0.00	0.00	0.00	0.01	0.01	0.01
$\sum_{1}^{15} PC$	99.99	99.99	99.99	99.97	99.97	99.97

Figure 7 illustrates the first 25 PCs (from normalised data) for 5 different damage cases with the same severity. 25% damage severity is applied at locations 3, 7, 11, 15, and 19 on the arch rib as shown in Figure 6 and PCs of each case were obtained. These PCs were plotted on the same graph as shown in Figure 7 where the “DL” refers to damage location. Distinguishable patterns are visible in Figure 7 which emphasise the fact that every damage location has a unique pattern of PCs which can be advantageously used in locating damage. Initial PCs represent the highest variations. The distinct patterns of these initial PCs on each location can favourably be used in neural network pattern recognition processes. Figure 8 shows the first 15 PCs (from non-normalized data) for 5 different damage severities at the same location. This Figure consists of 5 curves extracted from damage location 8, under 5%, 10%, 15%, 20% and 25% damage intensities. It is visible that the PC damage curves follow the same pattern but show an increment with the increase in damage intensity. This feature can be advantageously used in predicting damage severities.

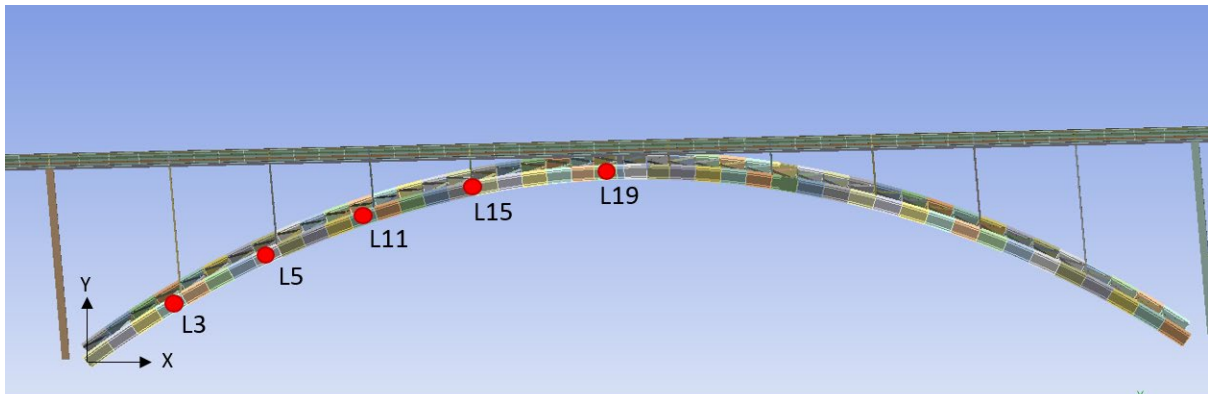


Figure 6: Damage locations on the rib for 25% damage test

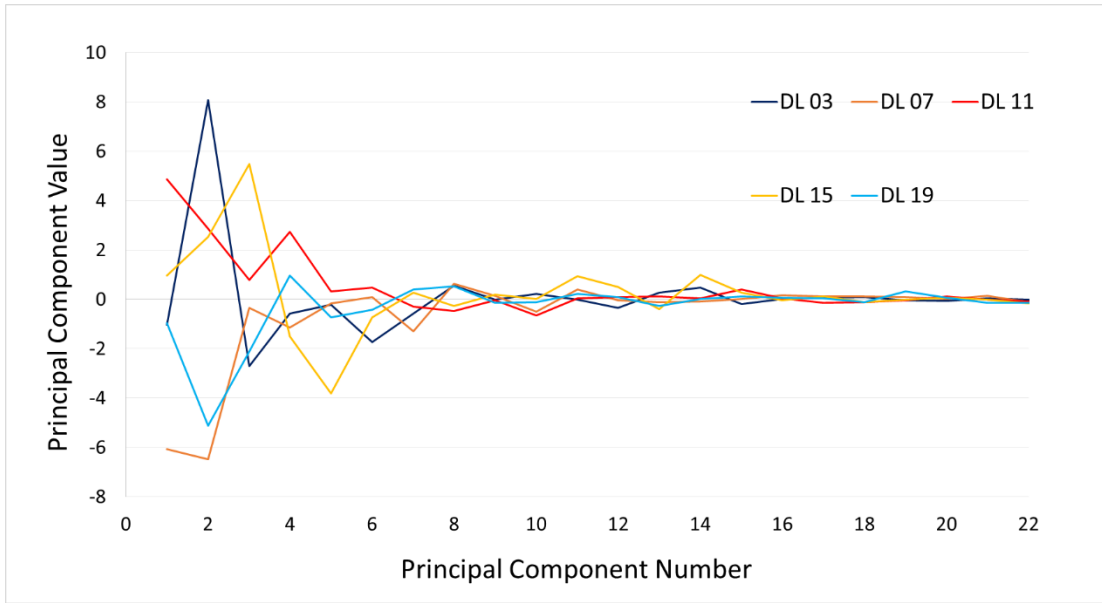


Figure 7: The first 25 PCs derived from normalised residual FRFs for 5 different damage

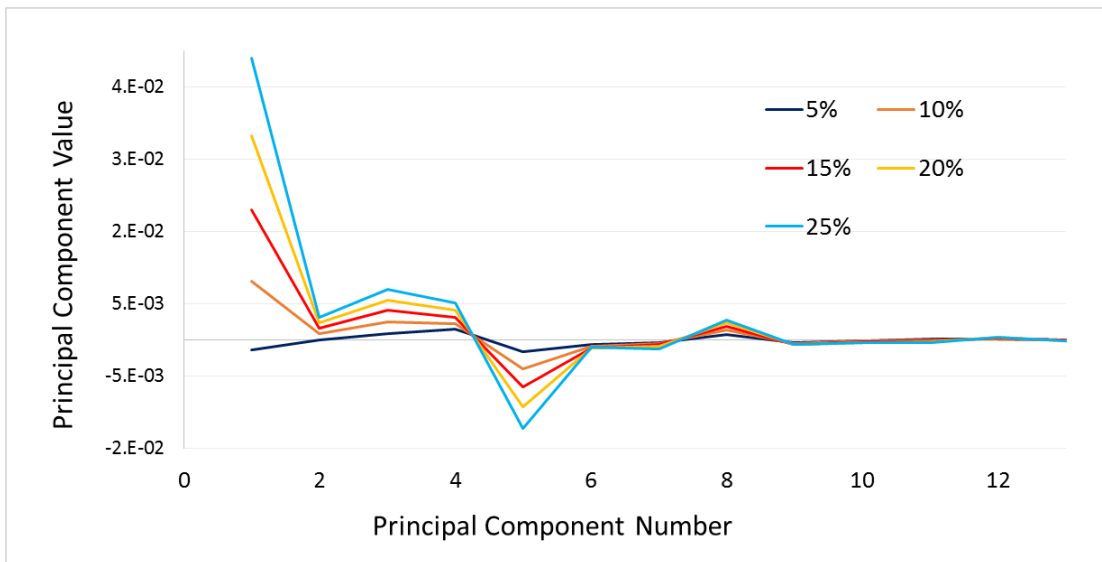


Figure 8: The first 15 PCs derived from non-normalised residual FRFs for 5 different damage severities at the same damage location

### 3. Methodology of Neural Network Based Damage Prediction Using Frequency Response Function

Feedforward multilayer neural networks are created to map the damage fingerprints to damage characteristics (location and severity). Neural network tools in MATLAB are used in this study to design and train all neural networks. The inputs to the networks are the most dominant principal components (PCs) of residual FRFs. To capture the benefit of unique individual characteristics of PCs derived from different sources of FRF (5 locations and summation)

separate networks are trained initially and the results of each network are fused to achieve the outcomes.

This study is developed for the arch rib of the Cold Canyon Bridge, where all the FRF data were collected from a validated numerical model developed on Abaqus finite element software. The rib was initially divided into 36 segments and damage was introduced to each of these segments creating 36 damage scenarios. Each data set was contaminated with 1%, 2% and 5% white Gaussian noise and with the original data (without noise) created 4 different noise level cases. For the network training process, 5 different damage severities (5%, 10%, 15%, 20%, and 25%) were considered at each of the damage location on the rib. This created a total of 720 damage scenarios ( $36 \text{ locations} \times 5 \text{ severities} \times 4 \text{ noise levels}$ ) to be treated as input data to the neural network for the training purposes.

FRF data extracted from a single sensor location on the rib contains 720 damage cases, and each damage case has 4455 frequency points (from all 3 directions). Further, 6 different FRF streams were considered with respect to 5 different sensor locations on the rib, and the summation FRF obtained by adding up the FRFs of all five measurement points. In addition, for each damage case, data were collected for all 3 directions at each sensor location. Then the whole FRF spectrum is considered by collecting all 3 direction specific FRFs sequentially. This creates a whole spectrum with 4455 nodes ( $1485 \times 3$ ) for each damage case. For the easiness of training and to obtain more precise results, each sensor location is treated separately via a different neural network. This means, 6 different neural networks are trained separately using 720 damage cases as inputs to train each network separately.

Before the data sets process through the networks, the input and the output data are normalised. Normalisation is important to make sure that the network accords equal weight to each sample. On the other hand, the input-output data must comply with the transfer function of the hidden layer and the output layer. This study uses the hyperbolic tangent sigmoid transfer function, which is compatible with -1 to +1 data range.

Since there are 36 different damage locations on the rib and 5 different severities, the number of unique patterns are counted as 180 ( $36 \times 5$ ) and 720 input cases are insufficient to identify such a large amount of unique patterns. On the other hand, data normalising is required to obtain unbiased, quality PCs. However, the normalised data hide the damage severity variations and hence make it difficult for the neural network to converge properly at the training. A two-

stage network system is therefore proposed to address these problems with satisfactory outcomes.

Two-stage neural network system comprises a pattern recognition network and a fitting network. The initial pattern recognition network is designed to recognise the damage substructure. Sub-structuring is done by splitting the total sample space into segments. Since the proposed method is tested on the arch rib, the total length of the rib was split into 5 segments as mentioned earlier (Figure 9).

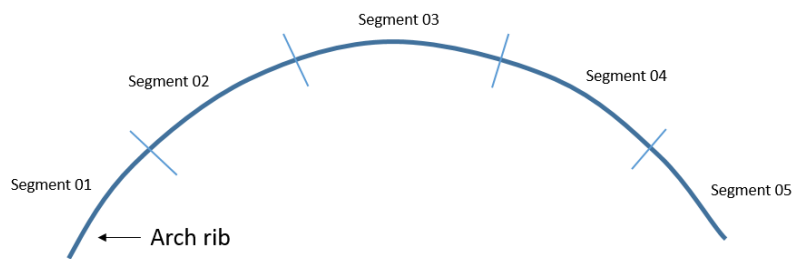


Figure 9: Segments along the length of the arch rib

Then the pattern recognition network is trained to identify the damage region (substructure). Inputs of pattern recognition network are PCs of normalised residual FRF data and the output is the damaged substructure number. The second stage comprises 5 different fitting neural networks designed on each segment (substructure) of the rib to identify the exact damage location and the severity of the damage. The inputs for this fitting networks are PCs of non-normalised residual FRF data and the outputs are the damaged location and the severity.

Figure 10 graphically explains the whole neural network system designed for the arch rib to determine the damage location and severity using FRF and ANN. The first neural network set consists of 6 individual networks starting from Location 01 until the Summation. Then, each of these 6 neural networks has 5 sub-networks called S1, S2, S3, S4 and S5. The subnetwork system of Location 01 is shown in the Figure 10. Only one sub group out of 5 sub-groups work at the second stage to determine the damage severity and exact location. Therefore, at the second stage, 6 sub-groups (one from every 6 networks) work simultaneously to determine the damage severity and location. These 6 subnetworks will give 6 outputs (severity and location) at the end of the second stage. These 6 outputs then become the inputs for the fusion network to obtain one single output, which is the final output for exact damage severity and location.

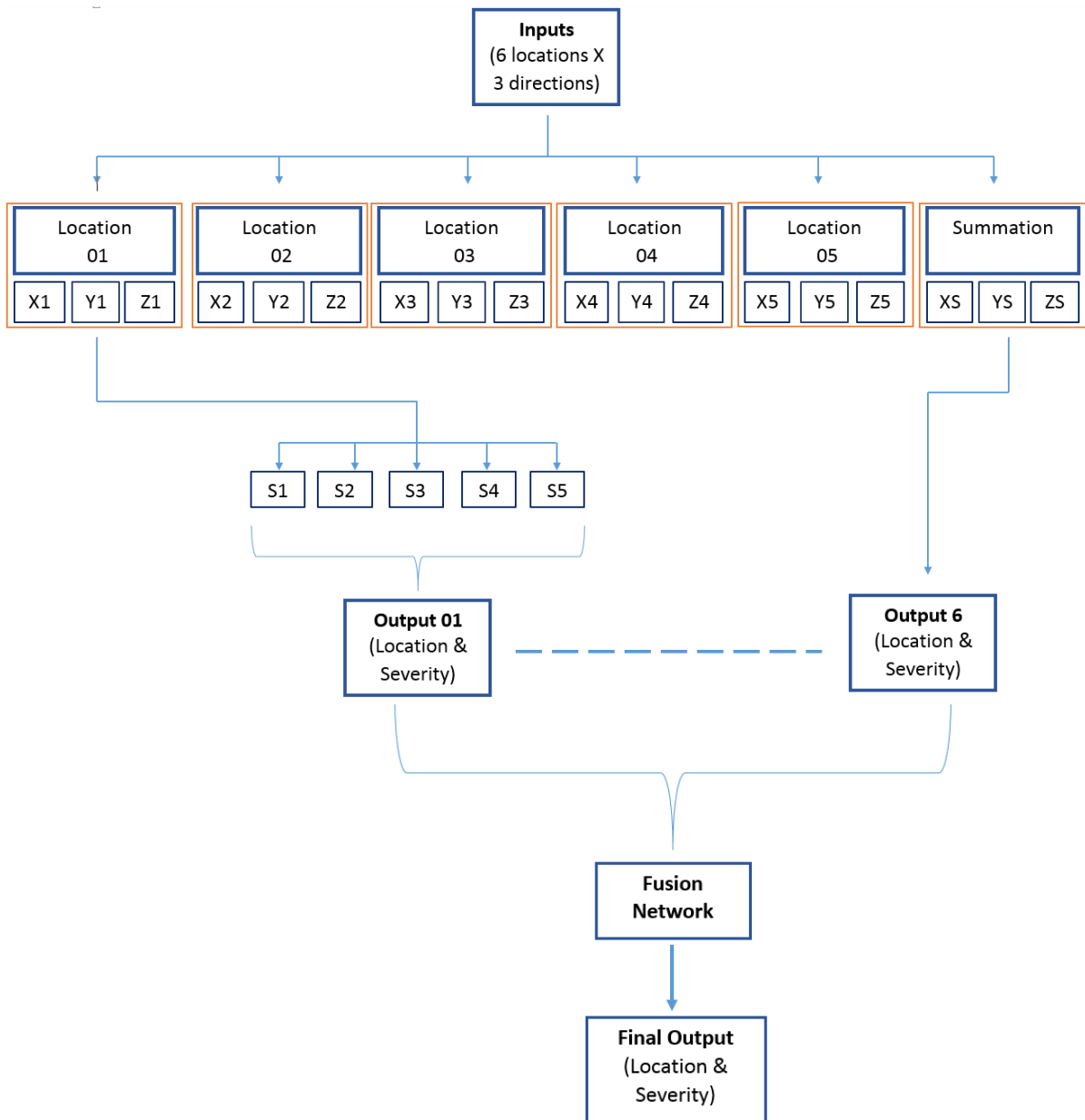


Figure 10: Neural network system

### 3.1 Artificial Neural Network Architecture

Stage 1 pattern recognition neural network was designed as a two-layer feedforward network, with sigmoid hidden and softmax output neurons (patternnet)<sup>44</sup>. This data set consists of 720 elements, each as input or target vector. There are 5 elements in each target vector to represent 5 segments associated with each input vector. The target/output consists of 1 or 0 scalar elements, with one element being 1 to represent the damaged segment and the other elements being 0. Each network has 25 input nodes for 25 PCs as variables and contains only one hidden layer with 15 nodes. The network was trained with scaled conjugate gradient backpropagation

(trainsecg) algorithm. Total input data was divided into 3 sets for training, validation and test. 70% of the original data was used for training, which recognises the relationship between the input-output data. 15% of the data is for validation and to make sure the network is generalising and stops training before overfitting. The remaining 15% is used as a completely independent data to test the trained network. Network configuration is graphically presented in Figure 11.

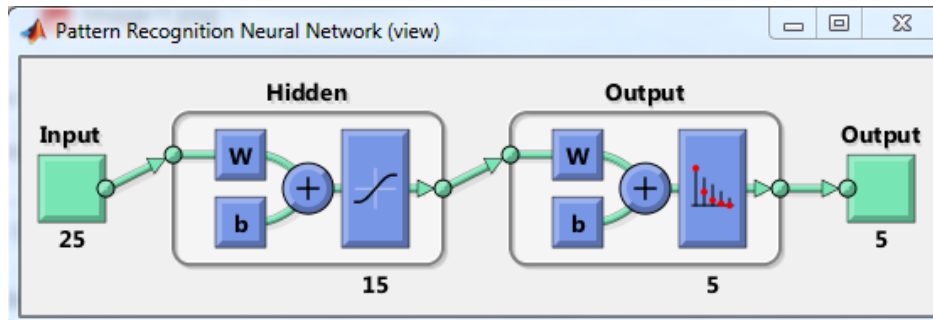


Figure 11: Fitting Network configuration

The network stops training manually or automatically after a certain number of iterations. The performance of the trained network can be checked by the confusion matrix. Figure 12 shows the confusion matrices for one of the trained networks of Location 01. The higher number of correct responses in the green squares and the low number of incorrect responses in the red squares confirm the accuracy of the trained network. The bottom right grey squares illustrate the overall accuracy. It is clear from Figure 12 that all training, validation and test matrixes show more than 97% overall accuracy in recognising the damaged substructure. All 6 networks were trained in the same manner and showed more than 95% accuracy in every trained network.



Figure 12: Configuration matrix classification network trained for 1X (X direction, sensor location 1)

Once the damaged substructure is identified the fitting neural network designed to that particular substructure is used to determine the damaged location and its severity. Each sub-network is designed with 15 input nodes; two hidden layers (15 and 5) and output nodes predicting the damage location and severity. Hyperbolic tangent sigmoid functions were the transfer function for all fitting networks.

Training is performed utilising the back-propagation conjugate gradient descent algorithm. As in the pattern recognition networks, the input data is initially divided into three sets; training, validation, and testing where 70% is for training, 15% for validation and 15% for testing. The network training stops when the error of the validation set increases while the error of the training set still decreases, which is the point when the generalisation ability of the network is lost and overfitting occurs. The design and operation of all neural networks are performed with

MATLAB. Once the network is trained, it is used to detect the damage location and severity of unknown damage cases. Figure 13 presents the network configuration for sub neural networks and Figure 14 shows the regression plots for trained L 01\_segment 01 (sensor location 1, substructure 1). The following regression plots display the network outputs with respect to targets for training, validation, and test sets. For a perfect fit, the data should fall along a 45 degree line, where the network outputs are equal to the targets. For this segment, the fit is reasonably good for all data sets, with R values in each case of 0.99 or above. All the sub neural networks are trained with available data before the test for unknown damage cases.

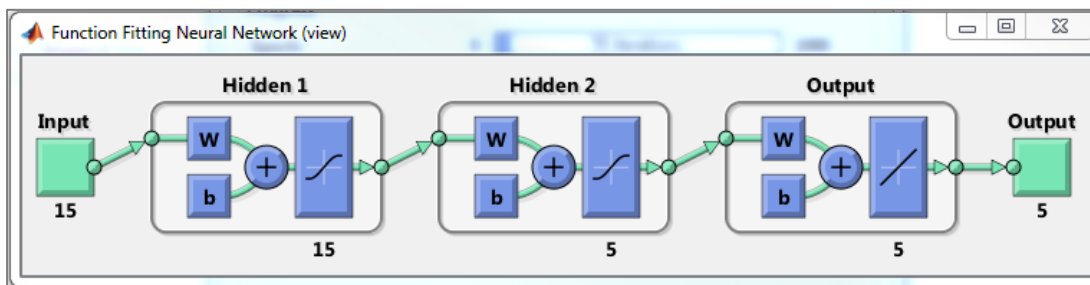


Figure 13: Regression network configuration

Once the whole network is well trained, it is capable of testing the unknown damages and retrieve damage severity and location. FRF is extracted from the damaged structure, and it is processed to obtain the residual FRF. The residual FRF is then fed into the pattern recognition network to identify the damaged substructure. Then the relevant sub-network decides the exact damage location and severity.

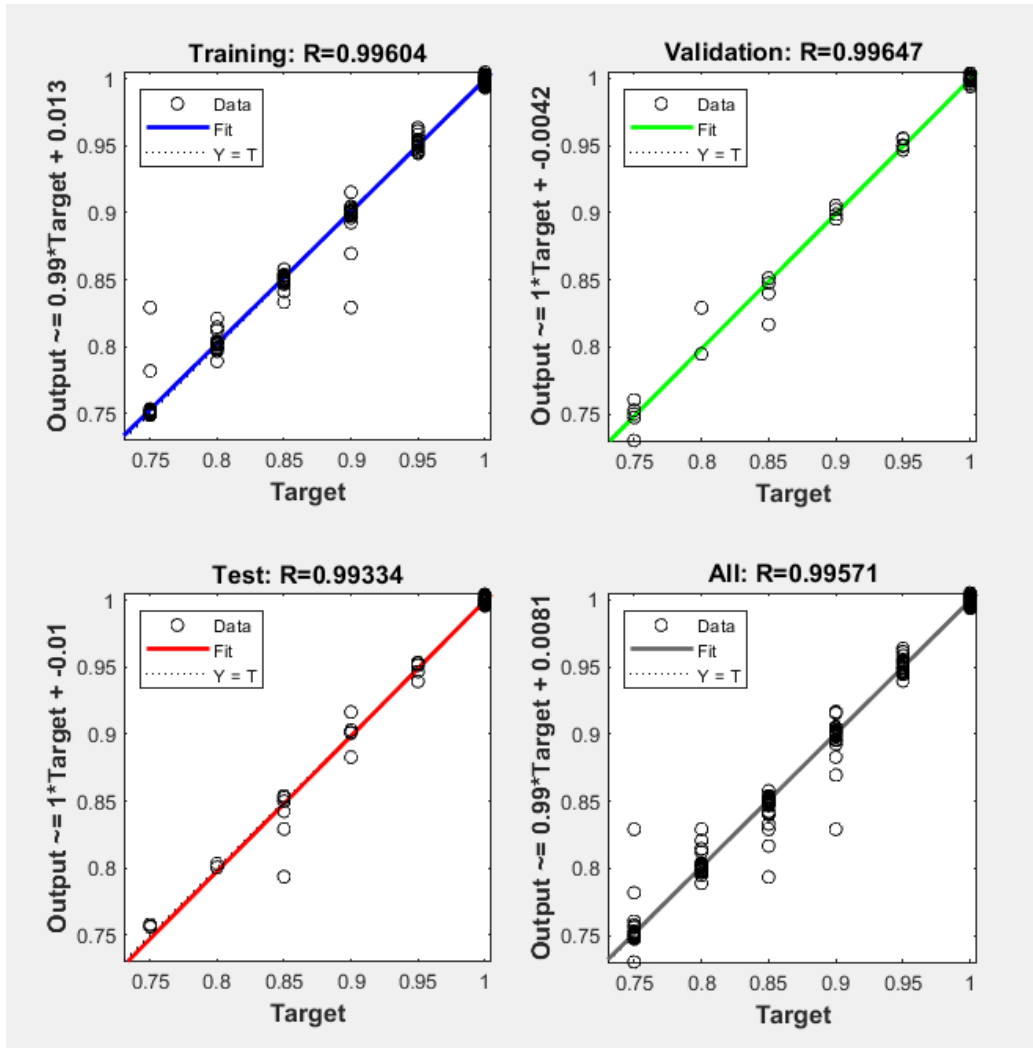


Figure 14: Regression plots of training, validation and test sets for trained subnetwork L1\_segment 01 (sensor location 1, substructure 1)

Network fusion is conducted as the last step to obtain a single output for unknown damage, which is tested on this trained network series. Fusion network is again a fitting neural network trained with 6 input variables and an output variable. The 6 input variables represent the 6 location specific neural networks, while the outputs are the location and the severity. Five fusion networks are designed for each substructure to obtain precise outcomes. All fusion neural networks were designed as two-layer feed-forward networks. There are 6 elements in each target vector to represent 6 sources (sensor locations). The target/output consists of one element with a numerical value to represent the severity of the damage. Each network has three hidden layers with 6, 3 and 1 nodes. The network was trained with Levenberg-Marquardt (trainlm) backpropagation algorithm. The total input data was divided into 3 sets as training, validation and test. 70% of the original data was used for training, which recognise the relationship between the input-output data. 15% is used to validate and to make sure the

network is generalising and stops training before overfitting. The last 15% is used as a completely independent test of network generalisation.

The whole network system is now ready to test for unknown damage cases. Since there are originally 5 sensor locations, for every unknown damage case, 5 FRF spectra can be collected; and with their summation, 6 FRF spectra can be generated. Therefore, for one unknown damage case 6 individually different FRF curves can be collected. These raw FRF data can be processed to obtain 6 residual FRFs which can be used as the inputs to train networks (stage01). Once the data is fed to stage 01 classification network, it classifies the damaged substructure and then decides the subnetwork to be called for further analyses. Then the non-normalized data is processed through the subnetwork to find the exact damage location and its severity. Since there are 6 individual networks expressing the final location and severity at this stage, the user can either accept the common answer among these 6 outputs or further process through the fused network.

## **4. Results**

### **4.1 Single damage cases**

In order to test the ability of the trained networks to precisely detect the damage location and severity of unknown damage, 8 damage cases were created on the FE model and the corresponding FRF data were extracted. These random damage cases are different from the damage cases used to train the networks. None of these test damage severities were used before in the neural networks for training or validation purposes.

Initially, FRF curvatures were calculated and then residual FRF was obtained. These residual FRFs are then converted to PCs to reduce their dimensions. Then these PCs are fed into the trained neural network system and the prediction was obtained.

Table 3 below shows the damage cases tested on a trained network with the expected and received outcomes. The damage location is given with respect to the X coordinate of the damaged element while the severity is given as a stiffness reduction percentage.

Table 4 presents the severity outcomes obtained for the 7 test cases when tested through the trained neural network. It is clear from the results that the proposed neural network architecture is capable of detecting the damage location and the severity of unknown damages on the arch ribs of arch bridges with acceptable accuracy.

Table 3: Test damage cases

Test Case	Case 01	Case 02	Case 03	Case 04	Case 05	Case 06	Case 07	Case 08
Damage segment	01	01	02	03	03	04	04	05
Exact location	X = 34.35m	X = 40.60m	X = 47.2m	X = 53.97m	X = 60.86m	X = 67.70m	X = 74.46m	X = 80.95m
Severity	7.5%	12%	18%	22.5%	7.5%	12%	18%	22.5%

Table 4: Outputs of severity (predicted severities)

Sensor location\ Test Case	Case 01	Case 02	Case 03	Case 04	Case 05	Case 06	Case 07	Case 08
Location 01	7.4%	11.91%	18.49%	22.42%	6.92%	23.05%	13%	23.04%
Location 02	6.75%	11.92%	18.06%	22.95%	6.88%	11.35%	10.15%	21.14%
Location 03	7.05%	12.06%	18.01%	22.2%	8.34%	12.83%	15%	20.42%
Location 04	7.67%	11.91%	18.62%	22.89%	7.24%	10.99%	12%	22.6%
Location 05	6.63%	11.85%	18.4%	21.98%	6.93%	11.91%	16%	22.49%
Summation	7.45%	11.9%	18.2%	23.4%	7.15%	11.5%	15%	22.19%

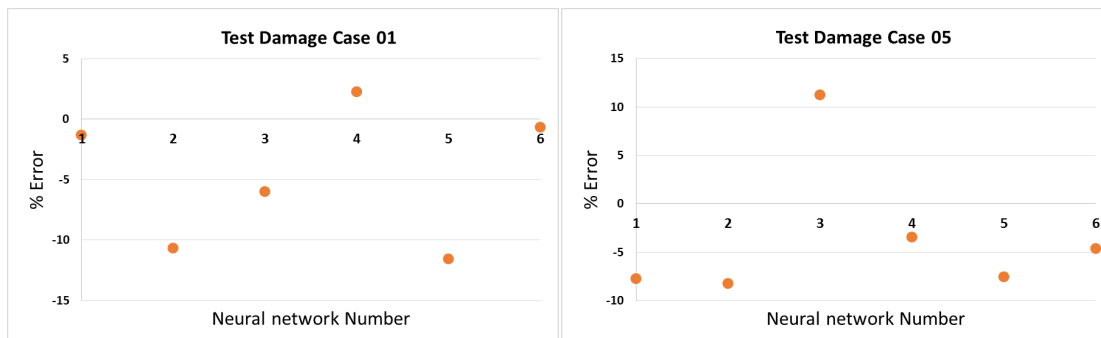


Figure 15: Results from all 6 neural networks for (a) Test damage case 01 (b) Test damage case 05

According to the results obtained at the end of two-stage neural network system, (as shown in Figure 15), it is clearly evident that, even though the same damage case was tested through all 6 separate neural networks, the prediction results of each network are different. When the above results are closely examined, it is observed that when the sensor station is close to the damage it is possible to obtain the better predictions compared to those obtained when the sensor stations are away from the damage location. For instance, damage case 01, which is originally at X = 34.35m is 5.65m distance from sensor location L01 (at X= 40m), while the other sensor

locations are further away from the damage location. The actual damage severity of case 01 is 7.5% and L01 network prediction was 7.4% which is the closest compared with predictions from other location networks. Except the closest sensor location, summation network too predicts the results accurately. For instance for damage case 01, the summation network prediction was 7.45% which is the closest result to actual damage severity. This behaviour can be further confirmed through the test damage case 05 results. The actual damage was at  $X=60.86\text{m}$ , which was close to sensor location 4 (L04) at  $X=54.5\text{m}$ . The network at L04 predicts the closest result to actual damage severity while summation network predicts the most acceptable result compared to any other single network. The percentage errors of prediction results of all 6 neural networks (5 locations and summation) for test damage case 01 and 05 are presented in Figure 15 (a) and (b) respectively.

This emphasises the importance of having well scattered sensor locations throughout the structure to capture the damages at any location. On the other hand this also highlights the importance of fusion network which logically decides the best match location and severity for damage in the structure.

The final results obtained from fusion network for damage severities and locations for 08 test damage cases are presented in Table 5 below.

Table 5: Outputs of severity

Test Case	Actual damage location	Network predicted location	Actual damage severity	Network predicted severity	Percentage error in severity prediction
01	$X = 34.35\text{m}$	$X = 34.3\text{m}$	7.5%	7.44%	0.80%
02	$X = 40.60\text{m}$	$X = 40.6\text{m}$	12%	11.9%	0.83%
03	$X = 47.2\text{m}$	$X = 47.2\text{m}$	18%	18.05%	0.27%
04	$X = 53.97\text{m}$	$X = 53.9\text{m}$	22.5%	22.3%	0.88%
05	$X = 60.86\text{m}$	$X = 60.8\text{m}$	7.5%	7.27%	3.06%
06	$X = 67.70\text{m}$	$X = 67.7\text{m}$	12%	11.52%	4.0%
07	$X = 74.46\text{m}$	$X = 74.4\text{m}$	18%	17.12%	5.0%
08	$X = 80.95\text{m}$	$X = 80.9\text{m}$	22.5%	22.51%	0.66%

## 4.2 Multiple Damage

It is possible to have multiple damages simultaneously during the service life of a structure. It is therefore necessary to check whether the neural network models developed for a particular structure is able to detect, locate and quantify multiple damage cases accurately. This study hence develops a procedure to enhance the capabilities of a single damage neural network to detect multiple damages.

Firstly, 80 random multiple damage cases were simulated and the relevant FRFs were obtained. These FRFs were then used to calculate the residual FRFs incorporating the healthy FRF spectrum. As mentioned earlier, PCA is essential for dimension reduction before using the FRF data in ANNs and therefore, PCA was performed. Having studied the contributions of initial PCs, 25 PCs were selected to use as the inputs to the neural network.

Five different damage severities at 36 locations can form a large number of multiple damage combinations. Therefore, for the testing purposes, this study processed a limited number of random damage cases. Thus, 80 dual damages (two severities at two locations) were simulated to create data for neural network training. With 4 noise levels (0%, 1%, 2% and 5%), the total number of observations for the neural network became 320.

Once the PCs are created, they were used as the input data while the output is the damage location and severity. Since this part of the study used only 320 observations to train the networks, it is inadequate to obtain the exact damage location (1 out of 36). Therefore, the rib was partitioned into 10 segments, instead of 36, and the output was created to retrieve the severity and the damage segment.

Network training is performed using multi-layer feedforward network backpropagation conjugate gradient descent algorithm. The design and operation of neural networks are performed with MATLAB. Once the network is trained, it is used to predict the damage location and severity of unknown damage cases. Figure 16 presents the network configuration for sub neural networks and Figure 17 shows the regression plots for the trained network. As mentioned earlier, 6 networks were initially generated incorporating the FRF data received from each sensor location. Results obtained from each network are fused to obtain the final damage location and severity.

Once the whole network is well trained, it is capable of testing the unknown damages and retrieve damage severity and location. Therefore, 5 multiple damage cases were randomly selected and tested through the trained neural network to obtain the damage severity and

location. The final results obtained from trained neural network for damage severities and locations for 05 test damage cases are presented in Table 6 below.

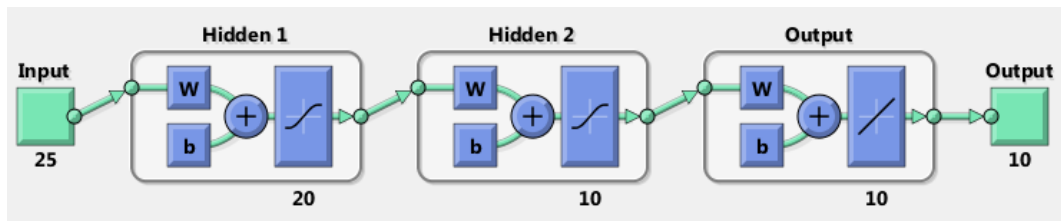


Figure 16: Regression network configuration

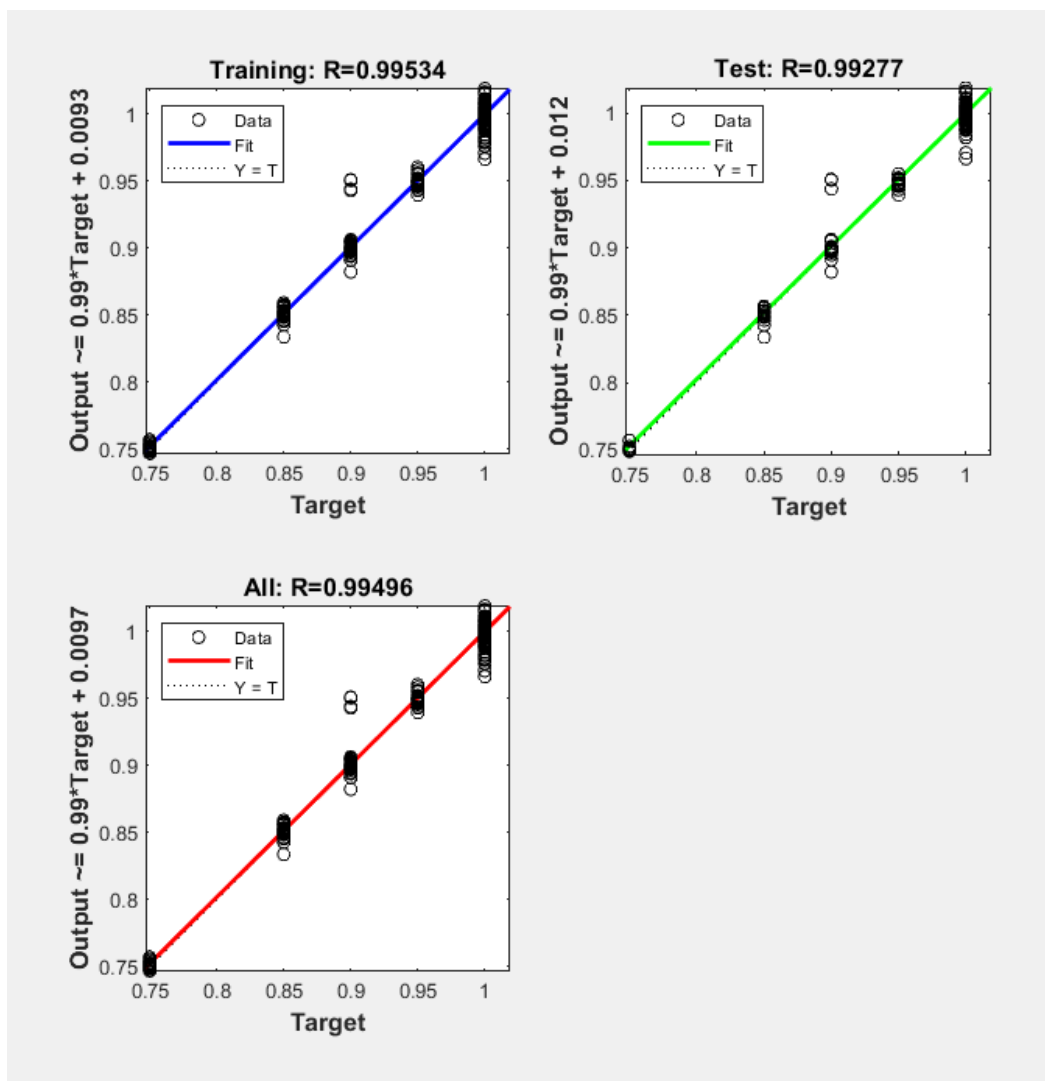


Figure 17: Regression plots of training, validation and test sets for trained subnetwork L1 (sensor location 1)

Table 6: Fusion neural network outcomes for multiple rib damage cases

Test Case	Actual damage location	Damaged Segments	Network prediction	Actual damage severity	Network predicted severity

01	X = 37.46m and X = 80.95m	Seg.2 and Seg.10	Seg.2 and Seg.10	10% and 10%	9.97% and 9.90%
02	X = 42.25m and X = 55.7m	Seg.3 and Seg.5	Seg.3 and Seg.5	10% and 25%	9.87% and 24.88%
03	X = 42.25m and X = 77.7 m	Seg.3 and Seg.8	Seg.3 and Seg.8	5% and 15%	5.13% and 15%
04	X = 53.97m and X = 72.8m	Seg.4 and Seg.6	Seg.4 and Seg.6	5% and 15%	4.65% and 15.03%
05	X = 59.1m and X = 62.5m	Seg.5 and Seg.6	Seg.5 and Seg.6	10% and 10%	9.57% and 9.86%

It can be seen from Table 6 that good results are obtained for Damage Case 1 in which the two damages are quite far apart as well as for Damage Case 5 in which the two damages are quite close to each other. According to the results presented in Table 6, it is noted that the FRF-ANN damage locating and quantifying scheme is potent enough to recognize the damages without any false alarms or missed information.

## 5. Conclusion

Arch bridge structures have complex vibration characteristics which pose a challenge for using available vibration based methods to detect damage in them. Even with modified vibration based methods the damage quantification process becomes harder and challenging due to the particular geometry of an arch bridge involving a curved arch rib and vertical members supporting the horizontal bridge deck. This research designed and successfully tested a technique that is capable of locating and quantifying the damage quite accurately in the arch rib which is the most important structural load bearing member in an arch bridge.

It uses the advantages of Frequency Response functions, Principal Component analysis in combination with artificial neural networks. The technique was illustrated through numerical examples for a wide range of single and dual damage cases in the rib of arch bridge. ‘Residual FRFs’ were selected as the damage indicators which were then dimensionally reduced using Principal Component analysis to enhance damage signature. A hierarchical network training based on fusion networking at the end is proposed to take advantage of individual characteristics of damage indicators derived from different sources (sensor locations). Finally, the successful results obtained for the tested damage cases (inverse problems) are presented, which emphasise the applicability of the proposed method to locate and quantify damage in the

ribs of arch bridges. It can be recommended that the well trained neural network for multiple damages can be effectively used to detect single as well as multiple damages on that particular structural element for which the network was trained. Further, this method can be followed to develop a similar one to locate and quantify damage in other structural members in the bridge (ex: columns, hangers and other members). A well trained network for each type of structural member can be an effective tool to predict the damage in that part of the structure. However, the proposed method was tested only for uncertainties such as measurement noise and thus further work needs to be done if temperature effects are to be considered. The actual noise contamination can be vary compared to numerical white noise. But due to the limitation of obtaining actual FRF data, this research study was limited to numerical analysis of the method. The difficulty of calculating FRF in a real bridge is acknowledged. It can be concluded that the procedure developed in this paper can be adopted in practice given the suitable conditions. The outcomes of this study will contribute towards the safe and efficient operation of arch bridges

#### References:

1. Rizos P, Aspragathos N, Dimarogonas A. Identification of crack location and magnitude in a cantilever beam from the vibration modes. *Journal of sound and vibration*. 1990;138(3):381-388.
2. Hong J-C, Kim Y, Lee H, Lee Y. Damage detection using the Lipschitz exponent estimated by the wavelet transform: applications to vibration modes of a beam. *International journal of solids and structures*. 2002;39(7):1803-1816.
3. Le NT, Thambiratnam D, Nguyen A, Chan TH. A new method for locating and quantifying damage in beams from static deflection changes. *Engineering Structures*. 2019;180:779-792.
4. Le NT, Thambiratnam D, Chan TH, Nguyen A. Damage quantification in beam-like structures from modal flexibility change. Paper presented at: 8th International Conference on Structural Health Monitoring of Intelligent Infrastructure (SHMII-08) 2017.
5. Shih HW, Thambiratnam DP, Chan THT. Vibration based structural damage detection in flexural members using multi-criteria approach. *Journal of Sound and Vibration*. 2009;323(3-5):645-661.
6. Cornwell P, Doebling SW, Farrar CR. Application of the strain energy damage detection method to plate-like structures. *Journal of sound and vibration*. 1999;224(2):359-374.
7. Contursi T, Messina A, Williams E. A multiple-damage location assurance criterion based on natural frequency changes. *Journal of vibration and control*. 1998;4(5):619-633.
8. Shi Z, Law S, Zhang L. Damage localization by directly using incomplete mode shapes. *Journal of Engineering Mechanics-ASCE*. 2000;126(6):656-660.
9. Law S, Shi Z, Zhang L. Structural damage detection from incomplete and noisy modal test data. *Journal of Engineering Mechanics*. 1998;124(11):1280-1288.
10. Nguyen K-D, Chan TH, Thambiratnam DP, Nguyen A. Damage identification in a complex truss structure using modal characteristics correlation method and sensitivity-weighted search space. *Structural Health Monitoring*. 2019;18(1):49-65.
11. Wang S, Zhang J, Liu J, Liu F. Comparative study of modal strain energy based damage localization methods for three-dimensional structure. Paper presented at: The Twentieth International Offshore and Polar Engineering Conference 2010.
12. Shih HW, Thambiratnam D, Chan TH. Damage detection in truss bridges using vibration based multi-criteria approach. *Structural Engineering and Mechanics*. 2011;39(2):187.
13. Wang FL, Chan TH, Thambiratnam DP, Tan AC, Cowled CJ. Correlation-based damage detection for complicated truss bridges using multi-layer genetic algorithm. *Advances in Structural engineering*. 2012;15(5):693-706.
14. Shih H, Thambiratnam D, Chan T. Damage detection in slab-on-girder bridges using vibration characteristics. *Structural Control and Health Monitoring*. 2013;20(10):1271-1290.

15. Wickramasinghe WR, Thambiratnam DP, Chan TH, Nguyen T. Vibration characteristics and damage detection in a suspension bridge. *Journal of Sound and Vibration*. 2016;375:254-274.
16. Wang Y, Thambiratnam DP, Chan T, Nguyen A. Damage detection in asymmetric buildings using vibration-based techniques. *Structural Control and Health Monitoring*. 2018;25(5):e2148.
17. Wang Y, Thambiratnam DP, Chan TH, Nguyen A. Method development of damage detection in asymmetric buildings. *Journal of Sound and Vibration*. 2018;413:41-56.
18. Nguyen A, Kodikara KTL, Chan TH, Thambiratnam DP. Deterioration assessment of buildings using an improved hybrid model updating approach and long-term health monitoring data. *Structural Health Monitoring*. 2019;18(1):5-19.
19. Doebling SW, Farrar CR, Prime MB, Shevitz DW. *Damage identification and health monitoring of structural and mechanical systems from changes in their vibration characteristics: a literature review*. Los Alamos National Lab., NM (United States). 1996.
20. Yi T-H, Yao X-J, Qu C-X, Li H-N. Clustering number determination for sparse component analysis during output-only modal identification. *Journal of Engineering Mechanics*. 2019;145(1):04018122.
21. Tang J. Frequency response based damage detection using principal component analysis. Paper presented at: 2005 IEEE International Conference on Information Acquisition 2005.
22. Huynh D, He J, Tran D. Damage location vector: A non-destructive structural damage detection technique. *Computers & Structures*. 2005;83(28-30):2353-2367.
23. Wang Z, Lin R, Lim M. Structural damage detection using measured FRF data. *Computer methods in applied mechanics and engineering*. 1997;147(1-2):187-197.
24. Sampaio R, Maia N, Silva J. Damage detection using the frequency-response-function curvature method. *Journal of sound and vibration*. 1999;226(5):1029-1042.
25. Maia N, Silva J, Almas E, Sampaio R. Damage detection in structures: from mode shape to frequency response function methods. *Mechanical systems and signal processing*. 2003;17(3):489-498.
26. Trendafilova I, Heylen W. Categorisation and pattern recognition methods for damage localisation from vibration measurements. *Mechanical Systems and Signal Processing*. 2003;17(4):825-836.
27. Dackermann U. *Vibration-based damage identification methods for civil engineering structures using artificial neural networks.*, University of Technology Sydney, Australia; 2009.
28. Caglar N. Neural network based approach for determining the shear strength of circular reinforced concrete columns. *Construction and Building Materials*. 2009;23(10):3225-3232.
29. Jiang S-F, Zhang C-M, Zhang S. Two-stage structural damage detection using fuzzy neural networks and data fusion techniques. *Expert systems with applications*. 2011;38(1):511-519.
30. Park J-H, Kim J-T, Hong D-S, Ho D-D, Yi J-H. Sequential damage detection approaches for beams using time-modal features and artificial neural networks. *Journal of Sound and Vibration*. 2009;323(1-2):451-474.
31. Bandara RP, Chan TH, Thambiratnam DP. Structural damage detection method using frequency response functions. *Structural Health Monitoring*. 2014;13(4):418-429.
32. Zapico J, Worden K, Molina F. Vibration-based damage assessment in steel frames using neural networks. *smart materials and structures*. 2001;10(3):553.
33. Ko J, Sun Z, Ni Y. Multi-stage identification scheme for detecting damage in cable-stayed Kap Shui Mun Bridge. *Engineering structures*. 2002;24(7):857-868.
34. Yi T-H, Li H-N, Sun H-M. Multi-stage structural damage diagnosis method based on energy damage theory. *Smart Structures and Systems*. 2013;12(3\_4):345-361.
35. Li H, Yi T, Gu M, Huo L. Evaluation of earthquake-induced structural damages by wavelet transform. *Progress in Natural Science*. 2009;19(4):461-470.
36. Ni Y, Zhou X, Ko J. Experimental investigation of seismic damage identification using PCA-compressed frequency response functions and neural networks. *Journal of sound and vibration*. 2006;290(1-2):242-263.
37. Sahin M, Sheno R. Vibration-based damage identification in beam-like composite laminates by using artificial neural networks. *Proceedings of the Institution of Mechanical Engineers, Part C: Journal of Mechanical Engineering Science*. 2003;217(6):661-676.
38. González MP, Zapico JL. Seismic damage identification in buildings using neural networks and modal data. *Computers & structures*. 2008;86(3-5):416-426.
39. Lee JJ, Yun CB. Damage diagnosis of steel girder bridges using ambient vibration data. *Engineering Structures*. 2006;28(6):912-925.
40. Xu H, Humar J. Damage detection in a girder bridge by artificial neural network technique. *Computer-Aided Civil and Infrastructure Engineering*. 2006;21(6):450-464.
41. Mehrjoo M, Khaji N, Moharrami H, Bahreininejad A. Damage detection of truss bridge joints using Artificial Neural Networks. *Expert Systems with Applications*. 2008;35(3):1122-1131.

42. Li J, Dackermann U, Xu YL, Samali B. Damage identification in civil engineering structures utilizing PCA-compressed residual frequency response functions and neural network ensembles. *Structural Control and Health Monitoring*. 2011;18(2):207-226.
43. Jayasundara N, Thambiratnam D, Chan T, Nguyen A. Vibration-based dual-criteria approach for damage detection in arch bridges. *Structural Health Monitoring*. 2019;18(5-6):2004-2019.
44. Mathworks. Neural Network Toolbox: User's Guide (R2018b) 2018; [www.mathworks.com/help/pdf\\_doc/deeplearning/index.html](http://www.mathworks.com/help/pdf_doc/deeplearning/index.html).